Adhesion Forces in Conducting Probe Atomic Force Microscopy

Alexei V. Tivanski, Jason E. Bemis, Boris B. Akhremitchev, Haiying Liu, and Gilbert C. Walker*

Department of Chemistry, University of Pittsburgh, Pittsburgh, Pennsylvania 15260

Received September 15, 2002. In Final Form: January 28, 2003

This paper examines how the adhesion force between a conducting probe and a conductive surface influences the electrical properties of conductive polymers. Conducting probe atomic force microscopy (CP-AFM) was employed. When a voltage is applied between the sample and the tip, an attractive electrostatic capacitance force is added to the adhesion force. The tip−sample capacitance force in the CP-AFM of polythiophene monolayers is described through theoretical modeling and compared with experiment. Experiments were performed in insulating organic solvent that decreased the adhesion force by approximately 10 times relative to measurements in air. The results for the adhesion force measurements as a function of applied bias show good agreement with the theoretical prediction. On the basis of the dependence of the adhesion force versus applied bias and the current−voltage characteristics of polythiophene, we conclude that characterization of electrical properties of conducting polymers using CP-AFM at a desired force requires knowledge of the adhesion force.

Introduction

Conductive polymers[1,2] are facilitating the development of numerous applications, such as antistatic coatings for electronic packaging,[3] light-emitting plastics,[4] and volatile organic gas sensors.[5] These polymers are also being investigated as fundamental building blocks for molecular electronics.[6−8] The development of many of these applications requires reliable methods to measure conductive properties at the nanoscale. Different approaches[9−18] have been attempted to investigate such properties of metal−molecule−metal junctions. To probe such junctions, one could use scanning tunneling microscopy (STM),[19−22] Kelvin force microscopy (KFM),[23−26] mechanically controllable break junction (MCB),[9] or conductive probe atomic force microscopy (CP-AFM).[11−13,27−32]

However, these STM, KFM, and MCB experiments have demonstrated that unambiguous contact to a nanoscale object is difficult to achieve and, what is more important, difficult to control. On the other hand, CP-AFM provides excellent control over mechanical contacts, especially for single-molecule studies. The utility of the AFM for electrical measurement stems directly from the ability of the AFM to operate on either conducting or nonconducting surfaces because position control is maintained by measuring the mechanical forces acting on the tip. Thus, the current can be measured independently of the tip−sample distance and the interaction force can be measured.

One of the main goals in measuring conductivity at the nanoscale is to obtain current−voltage characteristics of nanoscale devices. Since a conductive probe is placed into contact with the conductive polymer, there is a pressure with which the conductive probe pushes into the surface. As we will show later, this pressure depends on the applied external bias because the applied bias modifies the adhesion force. Variable pressures between the tip and the sample modify overlapping of electronic wave functions that participate in the process of injecting the carriers from the electrode (conductive probe) to the conductive polymer. This modifies the injection barrier and could

* To whom correspondence should be addressed. E-mail: gilbertw@pitt.edu.

(1) Heeger, A. J. *J. Phys. Chem. B* **2001**, *105*, 8475.
(2) Tamarat, P.; Maali, A.; Lounis, B. *J. Phys. Chem. B* **2000**, *104*, 1.
(3) Lerch, K.; Jonas, F.; Linke, M. *J. Chim. Phys. Phys.-Chim. Biol.* **1998**, *95*, 1506.
(4) Greenham, N. C.; Friend, R. H. *Solid State Phys.* **1995**, *49*, 1.
(5) Sotzing, G. A.; Briglin, S.; Grubbs, R. H.; Lewis, N. S. *Anal. Chem.* **2000**, *72*, 3181.
(6) Chen, J.; Reed, A.; Rawlett, A. M.; Tour, J. M. *Science* **1999**, *286*, 1550.
(7) Tour, J. M. *Polym. News* **2000**, *25*, 329.
(8) Tour, J. M. *Acc. Chem. Res.* **2000**, *33*, 791.
(9) Reed, M. A.; Zhou, C.; Muller, C. J.; Burgin, T. P.; Tour, J. M. *Science* **1997**, *278*, 252.
(10) Mujica, V.; Kemp, M.; Ratner, M. A. *J. Chem. Phys.* **1994**, *101*, 6849.
(11) Leatherman, G.; Durantini, E. N.; Gust, D.; Moore, T. A.; Moore, A. L.; Stone, S.; Zhou, Z.; Res, P.; Liu, Y. Z.; Lindsay, S. M. *J. Phys. Chem. B* **1999**, *103*, 4006.
(12) Cui, X. D.; Primak, A.; Zarate, X.; Tomfohr, J.; Sankey, O. F.; Moore, A. L.; Gust, D.; Harris, G.; Lindsay, S. M. *Science* **2001**, *294*, 571.
(13) Wold, D. J.; Frisbie, C. D. *J. Am. Chem. Soc.* **2001**, *123*, 5549.
(14) Frank, S.; Poncharal, P.; Wang, Z. L.; de Heer, A. *Science* **1998**, *280*, 1744.
(15) Leatherman, G. *J. Phys. Chem. B* **1999**, *103*, 4066.
(16) Dai, H.; Wong, E. W.; Lieber, C. M. *Science* **1996**, *272*, 523.
(17) Dorogi, M.; Gomez, J.; Osifchin, R.; Andress, R. P. A. *Phys. Rev. B* **1995**, *52*, 9071.
(18) Gittins, D. I.; Bethell, D.; Schiffrin, D. J.; Nichols, R. J. *Nature* **2000**, *408*, 67.
(19) Stranick, S. J.; Kamna, M. M.; Krom, K. R.; Parikh, A. N.; Allara, D. L.; Weiss, P. S. *J. Vac. Sci. Technol., B* **1994**, *12*, 2004.
(20) Cygan, M. T.; Dunbar, T. D.; Arnold, J. J.; Bumm, L. A.; Shedlock, N. F.; Burgin, T. P.; Jones, L., II; Allara, D. L.; Tour, J. M.; Weiss, P. S. *J. Am. Chem. Soc.* **1998**, *120*, 2721.
(21) McCarty, G. S.; Weiss, P. S. *Chem. Rev.* **1999**, *99*, 1983.
(22) Muralt, P.; Pohl, D. W. *Appl. Phys. Lett.* **1986**, *48*, 514.
(23) Takahashi, S.; Kishida, T.; Akita, S.; Nakayama, Y. *Jpn. J. Appl. Phys.* **2001**, *40*, 4314.
(24) Fujihira, M.; Kawate, H. *J. Vac. Sci. Technol., B* **1994**, *12*, 1604.
(25) Weaver, J. M. R.; Abraham, D. W. *J. Vac. Sci. Technol., B* **1991**, *9*, 1559.
(26) Sugimura, H.; Hayashi, K.; Saito, N.; Takai, O.; Nakagiri, N. *Jpn. J. Appl. Phys.* **2001**, *40*, 4370.
(27) O'Shea, S. J.; Atta, R. M.; Welland, M. E. *Rev. Sci. Instrum.* **1995**, *66*, 2508.
(28) Kelley, T. W.; Granstrom, E. L.; Frisbie, C. D. *Adv. Mater.* **1999**, *11*, 261.
(29) Kelley, T. W.; Frisbie, C. D. *J. Vac. Sci. Technol., B* **2000**, *18*, 632.
(30) Kelley, T. W.; Frisbie, C. D. *J. Phys. Chem. B* **2001**, *105*, 4538.
(31) Loiacono, M. J.; Granstrom, E. L.; Frisbie, C. D. *J. Phys. Chem. B* **1998**, *102*, 1679.
(32) Dai, H.; Wong, E. W.; Lieber, C. M. *Science* **1996**, *272*, 523.

10.1021/la026555k CCC: $25.00
Published on Web 02/19/2003

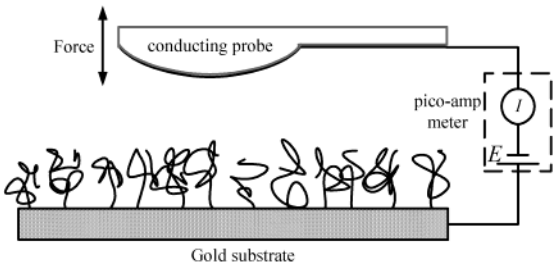

Figure 1. An idealized diagram of the apparatus used to measure currents using a force microscope.

dramatically change the conductive properties of the studied nanocontact. To obtain accurate conductive characteristics of the sample, it is necessary to perform measurements under constant pressure.

In this paper, we have performed studies of the conductive and adhesive properties of a polythiophene monolayer coupled between two gold electrodes using CP-AFM. A gold-coated conductive AFM probe served as one electrode, and the other was the gold substrate on which polymers had been grafted. Experiments were performed in an insulating solvent in order to decrease the adhesion force (the measured adhesion force in air was roughly 10 times larger than in organic solvent). Our results show that the adhesion force between conductive probe and conductive sample depends on the applied external bias. We find that inclusion of a capacitance force between conductive probe and conductive sample can explain the adhesion properties of our system and can be used to obtain the dependence of the adhesion force on applied external bias. We observed an increase in conductivity with increasing applied pressure. Our results show that under pressure, the contact area alone cannot explain the observed conductivity; the potential barrier for charge injection is reduced. Our results show that neglecting the adhesion forces contribution to the overall interaction force between conductive probe and the sample can provide significantly inaccurate estimates of the pressure between the conducting tip and the sample, and thus conductive properties of the nanoscale devices should be interpreted in light of this additional adhesion force. This effect would be even more pronounced in air, where adhesion forces are much larger.

Experimental Details

A commercial atomic force microscope (Molecular Force Probe, Asylum Research, Santa Barbara, CA) was used in this work. It was modified to permit conductivity measurements between the AFM probe and the sample. The idealized schematic representation of the experimental setup is shown in Figure 1. The capability of AFM to precisely position a conducting probe on the sample surface and measure the force between the probe and the sample was exploited. The probe tip was a commercial contact mode silicon nitride V-legged probe (Digital Instruments Inc., Santa Barbara, CA) coated with 50 nm of gold. Spring constants were calibrated using the Sader method[33,34] and typically had values of 0.1 nN/nm. Substrates for the polymer monolayers were 12 mm diameter 99.99% gold disks (Testbourne Ltd., Hampshire, U.K.). A commercial pico-amperometer (ChemClamp, Dagan Corp., Minneapolis, MN) was used to apply a bias to the conducting probe and enabled sensitive measurements of the current passing between the conductive probe and the conductive surface through the sample. Thus, by application of different biases, the current through the polymer layer can be measured as a function of tip−sample separation simultaneously with detection of the force between the tip and the surface. Force versus distance plots were obtained by moving the cantilever and pushing the tip against the surface. The difference between the signals in the two segments gives the vertical deflection signal, and hence the applied force. To decrease the probable effect of contamination of the tip over repeated measurements, when we started to see that the conductivity decreased under similar conditions or observed evolution of the force curves over repeated measurements, we stopped collecting data and changed the tip.

Chart 1. Undoped Poly(decyl-thiophene)

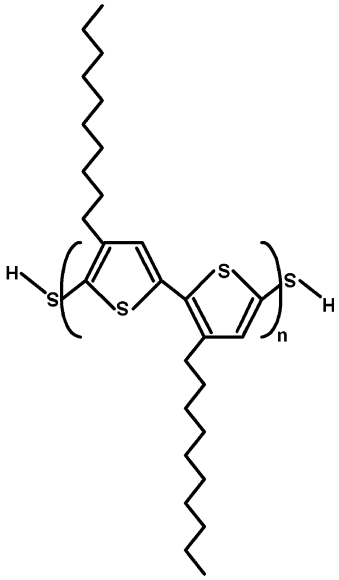

The polymer used in this work was undoped poly(decyl-thiophene) (PT) regioregular head-to-tail end functionalized with mercapto groups[35] (see Chart 1). Good electrical contacts between gold electrodes and the sample can be achieved through the sulfur−gold covalent chemical bond.

Gold substrates were cleaned for 12 h in piranha solution (20% H_2O_2, 80% H_2SO_4). *Caution! Piranha solution has very strong oxidizing power and is extremely dangerous to handle in the laboratory; gloves, goggles, and face shields are needed for protection*. Tips were cleaned in piranha solution for 2 h. Tip holder and sample holder were cleaned in a detergent solution (10% FL-70, 90% H_2O) for 2 h. Then, tips, tip holder, and sample holder were thoroughly rinsed in deionized water and dried in a stream of nitrogen gas.

Polymer and 1,4-benzene dimethanethiol (BDT) (Aldrich) were grafted to gold surfaces as follows. To prepare samples, the undoped PT and BDT were dissolved in freshly distilled tetrahydrofuran (THF) at concentrations of 10 μM and 1 mM, respectively. The gold disks were soaked in the polymer solution for about 30 h for PT and 12 h for BDT. The disks were next soaked in freshly distilled THF for 12 h, and finally $NaBH_4$ (Aldrich) was added in excess to the solution and left for 30 h. After incubation, the substrates were cleaned of excess polymer or BDT by sonication in THF and dried in a stream of nitrogen gas. The sodium borohydride was added to reduce the disulfide linkages, which formed during storage, between polymer chains and between BDT molecules. During these steps, the solution and surface were kept in enclosed weighing bottles. All these steps were performed at room temperature. All samples were used within 2 days of preparation. The conductivity measurements using CP-AFM were performed in insulating, tetradecane solvent. The polymer was characterized using gel permeation chromatography (GPC).[36] GPC of polythiophene reduced by addition of $NaBH_4$ was collected relative to the calibration with polystyrene standards. An ellipsometer (L117, Gaertner Corp., USA) was used to determine the film thickness of the polythiophene monolayer. The measurements were done at a 70°

(33) Sader, J. E. *Rev. Sci. Instrum.* **1999**, *70*, 3967.
(34) Sader, J. E. *J. Appl. Phys.* **1998**, *84*, 64.
(35) Liu, H.; Waldeck, D.; Walker, G. Synthesis of dithiol terminated polythiophene. To be submitted.
(36) Cooper, A. R. *Determination of Molecular Weight*; Wiley: New York, 1989; pp 263−300.

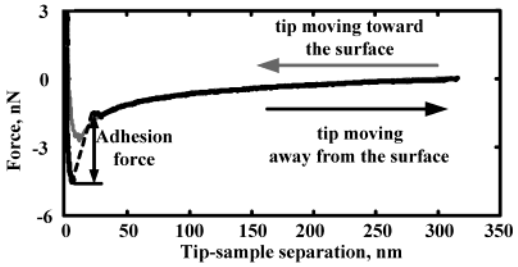

Figure 2. The long-range attraction force and the jump-off event during breaking of contact between the tip and the polymer.

incident angle, using a He−Ne laser (633 nm) as the light source. Samples to be studied by ellipsometry were examined within minutes after grafting of the polymer.

Results and Discussion

GPC provided number-average molecular weight M_n = 26 000 Da, weight-average molecular weight M_w = 46 000, and polydispersity index PI = 1.8. The polythiophene monomer's molecular weight is 222 Da, and the monomer length is 3.8 Å. Thus the approximate number of the monomers in the polymer chain was 110 repeat units. The unperturbed radius of gyration R_g was estimated to be 2.3 nm using the following equation: $R_g = l(M_w/6M_0)^{1/2}$. The thicknesses of self-assembled polythiophene monolayers were approximately 2.8 nm, as determined by the ellipsometry technique. This thickness is somewhat larger than the estimated value of the unperturbed radius of gyration; thus we conclude the polymer chains are in a slightly extended, brushlike state at the surface.

A typical force plot for the conductive measurements is shown in Figure 2. In this force plot, the applied bias was −3 V. The zero force is selected as the force when the tip was far away from the surface, which can be considered constant for the different biases since electrostatic interactions become negligible at such distance. The gray line corresponds to the force during the approach of the tip to the surface. When the tip−sample separation reaches a point where the gradient of interaction force is greater than the spring constant of the cantilever, the tip jumps into contact with the surface. The tip continues to push against the surface, increasing the tip−sample force until the controller switches the direction of the tip motion. Force registered during subsequent motion is illustrated by the black line. The tip remains in contact with the surface until the force of adhesion is exceeded; the tip jumps away to a distance that is equal to the force of adhesion divided by the spring constant of the cantilever. This jump-off event is shown by the dashed line. The interaction force between the tip and underlying sample at their contact is considered to be equal to the sum of two forces, the adhesion force and the force with which the cantilever pushes the tip into the sample. The force applied by the tip is measured by recording the cantilever deflection during the entire approach−withdrawal cycle, while the adhesion force is measured during the jump-off event only.

The results show the presence of a long-range force. This force depends on the tip−sample separation and, as will be discussed later, on the applied bias. The long-range forces disappeared with no bias applied; thus the electrostatic nature of these forces is implicated.

Now we consider the origin of the electrostatic force. If a voltage is applied between two different conducting materials (in this case the conducting tip and the conducting sample), then an attractive force is added to the overall forces experienced by the probe. The difference in potential V between the tip and the sample produces an electrostatic energy of the form

$$E_{elec} = \frac{1}{2}CV^2$$

where C is the capacitance between the tip and the sample. This can be differentiated with respect to the tip−sample separation, z, to give the capacitance force between them:

$$F_{capac} = -\frac{1}{2}\frac{dC}{dz}V^2$$

It is important to point out that even in the absence of an applied potential, some capacitance force may still exist due to the contact potential difference between different materials.[37]

The electrostatic force between the probe and the sample has two contributions: one is from the cantilever body and another is from the tip. The electrostatic force between the conductive cantilever body and conductive sample system is typically about 50−100 pN and has very weak distance dependence,[38] and since our forces are much larger, we will neglect the electrostatic force acting on the cantilever body.

The tip shape can be modeled as a truncated cone ended by a spherical apex and with a total length $L_{tip} = 5\ \mu$m, half angle $\theta = 35°$, and apex radius $R = 100$ nm. We will use the method of Hudlet et al.[37] to approximate the capacitance force between the tip and the surface. For small distances ($d < R$), the force depends on the tip−sample separation as d^{-1}, which is the same as the force (for $d < R$) between a sphere and a semi-infinite conductive plane.[38] For distances $R < d < L$, the force has a logarithmic dependence on the tip−sample separation, and this can be related to the uniformly charged line model.[39] Since the jump-off event occurs at rather a small tip−sample separation, we can approximate our capacitance force as

$$F_c(d) = -\pi\epsilon_0\epsilon_r V^2\frac{R}{d} \quad (1)$$

where ϵ_r is an effective dielectric constant of the polymer−solvent system that is taken to be 2.5.

Figure 3A represents experimental data (black dots) and calculated values (gray line) of the force for the approach data at an applied bias of −3.5 V as a function of tip−sample separation. Calculations were performed using eq 1 for the electrostatic capacitance force as a function of tip−sample separation for a fixed applied bias. Good agreement with experimental data has been found. Equation 1 also shows that force depends quadratically on the applied bias. Figure 3B shows how the force on the tip depends on the applied bias, when the tip is not in contact with the surface. The dots represent experimental data, and the solid line represents a theoretical prediction given a tip−sample separation of 30 nm; diamonds represent experimental data, and the dashed line represents the theoretical prediction given that the tip is 50 nm away from the surface. Here the zero force is the force on the tip when it is far away from the surface. Good agreement between the theory and experimental results provides additional confirmation that long-range forces

(37) Hudlet, S.; Saint Jean, M.; Guthmann, C.; Berger, J. *Eur. Phys. J. B* **1998**, *2*, 5.
(38) Belaidi, S.; Girard, P.; Leveque, G. *J. Appl. Phys.* **1996**, *81*, 1023.
(39) Hao, H. W.; Baro, A. M.; Saenz, J. *J. Vac. Sci. Technol., B* **1991**, *9*, 1323.

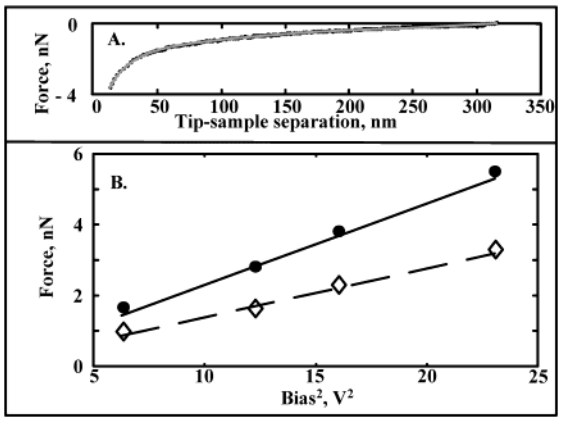

Figure 3. Upper panel (A): Theoretical (gray line) and experimental (black dots) force dependence on tip−sample separation. Lower panel (B): Experimental ((◊) 50 nm and (●) 30 nm tip sample separation) and theoretical ((solid line) 30 nm, (dashed line) 50 nm) dependence of the force on the applied bias.

acting on the conductive probe can be described using the capacitance model. Thus we can now attempt to describe adhesion forces between the conductive probe and the sample using our capacitance model.

To calculate the adhesion force, we first have to estimate the tip−sample separation at which the tip jumps away from the surface. This event occurs when the gradient of adhesion force becomes less than the spring constant of the cantilever. Thus, this distance can be determined from the following equation:

$$\left(\frac{dF}{dz}\right)_{z=z_{adh}} = k_c \tag{2}$$

By combining eqs 1 and 2, one obtains an expression for the adhesion force as a function of applied bias:

$$F_{adh} = -V\sqrt{\pi R \epsilon_0 \epsilon_r k_c} \tag{3}$$

Equation 3 shows that the adhesion force depends linearly on applied bias. For our particular system, the dependence of the adhesion force on the applied bias is predicted to be linear with a slope of −0.8 nN/V in the negative bias region and 0.8 nN/V in the positive. Figure 4A shows the adhesion force (dots with error bars as the standard deviation of a series of repeated measurements) as a function of applied bias.

It is important to point out that magnitudes for the adhesion force depend on both electrostatic and nonelectrostatic contributions. As can be seen in the figure, the adhesion force is not zero at an applied bias of 0 V but has a value of $F_{adh}^{int} = 0.45$ nN. This intrinsic adhesion force of the sample has been added to the calculated dependence.

The experimental dependence of the adhesion force in the negative bias region deviates from linear behavior; it shows a peak in the range of applied biases from approximately −1.2 to −2.2 V. The undoped polymer chain is nonconductive until it oxidizes at applied biases more negative than approximately −1.8 V, which corresponds to the approximate maximum of the adhesion deviation peak. Figure 4B shows the adhesion force (symbols) for 1,4-benzene dimethanethiol as a function of applied bias. As will be discussed below, this sample is not expected to undergo redox transitions in this range of applied bias. As can be seen from the figure, the experimental dependence of the adhesion force in the negative bias region does not deviate from linear behavior, as compared to the

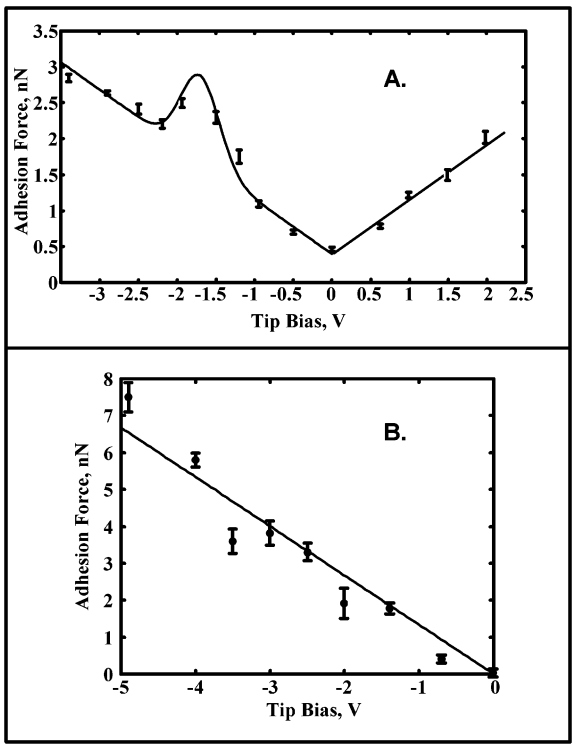

Figure 4. Upper panel (A): Adhesion force as a function of applied bias. Data are represented by dots with error bars, the line in the positive bias region was theoretically predicted by the first two terms of eq 3.1, and the line in the negative bias region is a fit to the data using all terms of eq 3.1. Lower panel (B): Adhesion force (symbols) and the best fit line for the 1,4-benzene dimethanethiol sample.

polythiophene results. Our cyclic voltammograms (Figures S1 and S2 of the Supporting Information) show that this polythiophene oxidizes (see Figure S2) at approximately 0.7 V relative to the Ag/AgCl electrode. While the exact voltage of the CP-AFM oxidation peak remains to be discussed below, we conclude that the peak in Figure 4 originates in an oxidation state change of the polymer layer under the tip. In the CP-AFM experiments, the surface with grafted polythiophene is oxidized when the surface is at a positive potential relative to the tip. If the oxidation potential of the polymer chain has a Gaussian distribution and we assume that the additional capacitance due to the presence of positive charges is directly proportional to their number, then the expression of the adhesion force (eq 3) will be

$$F_{adh} = -V\sqrt{\pi R \epsilon_0 \epsilon_r k_c} + F_{adh}^{int} + A\ \exp[-(V - V_0)^2/2\sigma^2] \tag{3.1}$$

The solid line in Figure 4 represents a fit of the adhesion force data using eq 3.1. The fit puts the center of the Gaussian at $V_0 = -1.7$ V and its standard deviation at $\sigma = \pm 0.25$ V (A is a scaling factor).

This effect can be explained qualitatively as follows. When the polymer chain oxidizes, electrons will be removed from the molecule to the gold substrate; thus the chain becomes positively charged. These holes transport through the polymer backbone toward the negatively charged tip; thus the effective width of the capacitor between the tip and the sample has been decreased, and that in turn increases the interaction force. The force increases until the holes move to conjugated energy levels that are spatially closest to the tip, providing the maximum force because this configuration represents the smallest

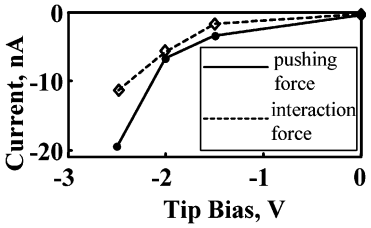

Figure 5. Current versus voltage, under constant interaction force and constant pushing force. In both cases, the force magnitude is 7.5 nN.

width of the capacitor. When the bias is high enough, holes overcome the potential barrier between the tip and the polymer and move to the tip; thus current starts to flow, corresponding to the maximum of the peak at the adhesion force. Because positive charges are now removed from the chain, the effective width of the capacitor decreases and thus the interaction force decreases. After positive charges are removed from the polymer backbone, the chain can oxidize again; because there is no potential trap at the interface between the conductive tip and the polymer, the holes will not be stored near the tip and on a time-average the effective distance between capacitor plates is larger than when positive charges are trapped by the potential. Thus, when the absolute value of the bias is increased, the added additional adhesion force diminishes and the adhesion force can be represented again using eq 3.

Our cyclic voltammograms exhibit an oxidation peak at 0.7 V relative to the Ag/AgCl electrode with a standard deviation of ±0.05 V that is 5 times smaller than we observed at the adhesion force peak. The origin of this discrepancy is probably the energetic distribution of polymer highest occupied molecular orbital (HOMO) states. In conjugated polymers, conformational variations will produce different conjugation lengths, which will vary the energy of the carrier. More experimental work and theoretical modeling are required to better understand this behavior.

When a conductive probe contacts the polymer, there is a pressure with which the probe pushes into the surface. Pressures between the tip and the sample modify the overlap of electronic wave functions that participate in the injection of carriers from the electrode (conductive probe) to the conductive polymer. This pressure modifies the injection barrier and dramatically alters the observed conductive properties of the studied molecule. Thus, to perform accurate characterization of the conductive properties of the sample, such measurements should be performed under constant pressure. Since the experiments reported here utilized the same cantilever, we can assume that the pressure under the tip is proportional to the interaction force. It is essential to point out that measurements under a constant interaction force and measurements under a constant force with which the cantilever pushes the tip into the sample provide different results, since part of the interaction force is an adhesion force that is bias dependent. The difference between measurements with constant interaction and constant applied force is illustrated in Figure 5. This figure shows two current−voltage ($C-V$) characteristics of the polythiophene molecules under constant interaction and constant pushing force. A nonconstant difference between the $C-V$ curves arises because the adhesion force is bias dependent.

Figure 6 shows the current−voltage dependence for the gold−polythiophene−gold system at a constant interaction force between the tip and the sample, for the different

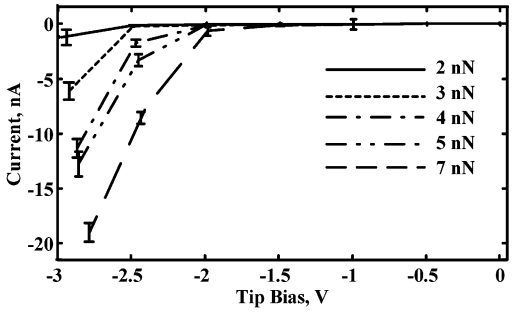

Figure 6. Current dependence on voltage for the gold−polythiophene−gold system at five different constant interaction forces between the tip and the sample.

interaction forces (ranging from 2 to 10 nN). Each line represents one value of the force.

The importance of the interaction force between the tip and the sample is clearly shown by this figure; when more force is applied onto the sample, the conductivity is increased, probably because the width of the potential barrier for injection from the gold electrode into the polymer is decreased. Such changes can be qualitatively understood by using simple ideas about tunneling through the potential barrier created at the interface between the gold electrode and the sample. The probability for the charge carrier to travel through such a potential barrier would decrease exponentially with both the width and the height of a potential barrier. When more pressure is applied, the spatial separation between the conductive probe and the sample is decreased; this in turn will increase the current. On the other hand, the electrodes become closer to each other, and thus the overlap of the electronic wave functions participating in injection is increased. Thus the potential barrier is decreased, and this in turn will also increase the current.

Another observation from this figure is that for applied biases less in absolute value than 1.5−2 V the current is very small, and for larger biases it increases significantly. To understand this, we consider a hole injection mechanism between the Fermi level of the gold electrode and the HOMO energy level of the conductive polymer, closest to the Fermi level. We will use Fowler−Nordheim theory for the charge injection mechanism[40,41] between metal electrode and polymer semiconductor. Based on Ouisse's work,[42] an analytical expression for the effective Fowler−Nordheim barrier between metal electrode and semiconductor is

$$\Phi_{\text{eff}} = (I^{3/2} - E_{\text{Au}}{}^{3/2})^{2/3} \qquad (4.1)$$

Here E_{Au} is the work function of the gold electrode, and I is the ionization potential of the polythiophene. On the basis of the cyclic voltammograms (CVs), the ionization potential relative to the vacuum is $I = 5.4$ eV. This is the value obtained by ab initio Hartree−Fock calculations[43] when there is an average 20° torsion angle between adjacent thiophene rings. The work function of gold is $E_{\text{Au}} = 5.2$ eV. By substituting these values into eq 4.1 for an effective injection potential for the holes one would obtain $\Phi_{\text{eff}} = 0.8$ eV. This predicted barrier is significantly smaller than observed in the CP-AFM experiments, though we note that contact resistance and other limiting factors have been neglected and may account for the discrepancy.

(40) Yang, Y.; Pei, Q.; Heeger, A. J. *J. Appl. Phys.* **1996**, *79*, 934.
(41) Parker, I. D. *J. Appl. Phys.* **1994**, *75*, 1656.
(42) Ouisse, T. *Eur. Phys. J. B* **2001**, *22*, 415.
(43) Bredas, J. L.; Street, G. B.; Themans, B.; Andre, J. M. *J. Chem. Phys.* **1985**, *83*, 1323.

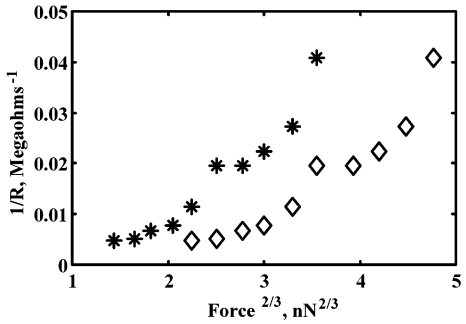

Figure 7. Conductivity as a function of contact area, at biases of −2.5 V (diamonds) and −3 V (stars).

The predicted potential barrier for the electrons can be calculated in the same way as for the holes. We consider a charge injection mechanism between the Fermi level of the gold electrode and the lowest unoccupied molecular orbital (LUMO) energy level of the conductive polymer, closest to the Fermi level. The effective Fowler−Nordheim barrier between metal electrode and semiconductor is

$$\Phi_{\text{eff}} = (E_{\text{Au}}{}^{3/2} - \text{EA}^{3/2})^{2/3} \qquad (4.2)$$

Here EA is the electron affinity of the polythiophene. On the basis of the CVs, the electron affinity relative to the vacuum is EA = 3 eV. By substituting these values into eq 4.2 for an effective injection potential one would obtain $\Phi_{\text{eff}} = 3.6$ eV. Thus this sample is not expected to undergo redox transitions in the range of applied bias from 0 to 2.5 V.

Another possible argument for the conductivity of the polymer chain increasing with increasing pressure applied onto the sample is that the contact area between the conductive probe and the sample also increased. We can use Johnson−Kendall−Roberts (JKR) theory[44] to relate the contact area and the adhesion force. If the probe is treated as an elastic sphere and the sample as an elastic flat surface, then according to JKR theory[44] the contact area just before the jump-off between a sphere of radius *R* on a flat surface would depend on the interaction force as follows:

$$a^2 = \left(\frac{R}{K} F_{\text{adh}}\right)^{2/3} \qquad (5)$$

where *K* is the effective elastic modulus of the conductive probe and the sample. Figure 7 shows how the conductivity at biases of −2.5 and −3 V depends on the adhesion force to the $^2/_3$ power. If the increase in the contact area with the increase of the adhesion force is fully responsible for the increase in conductivity, we should observe a linear dependence. The observed dependence is clearly nonlinear. Therefore, a contribution to conductivity that goes beyond contact area is relevant.

As protocol for the electrostatic characterization of the nano-objects using CP-AFM, we suggest the evaluation of the adhesion force as a function of applied bias. One should perform all conductive measurements under the same interaction force, recognizing that it is the sum of the adhesion force and the force applied on the tip. A suitable technique for this protocol would be detection of the force as a function of tip−sample separation simultaneously with current detection as a function of tip−sample separation.

Conclusions

In this work, we have measured the conductance of nanocontacts between gold-grafted polythiophene monolayers and a conductive tip in tetradecane solvent under different applied loads using CP-AFM. We have shown theoretical and experimental results of how the electrostatic part of the adhesion force depends on the applied external bias. Experiments have been performed in insulating organic solvent that decreased adhesion force approximately 10 times relative to the air measurements. Results showed good agreement with the analytical expressions of the capacitance force as a function of applied bias and tip−sample separation both at the jump-off event and at long-range forces. We observed an increase in conductivity with increasing applied pressure. Under pressure, the contact area alone cannot explain the observed conductivity; the potential barrier for charge injection is reduced. On the basis of the adhesion force versus applied bias dependence and current−voltage characteristics of polythiophene molecules, we conclude that characterization of electrical properties of conducting polymers using CP-AFM requires taking into account an offset in the interaction force determined by the adhesion force.

Acknowledgment. We gratefully acknowledge support from ONR (N0001-02-D327) and NSF (CHE 9816820 and PHYS 0103048).

Supporting Information Available: CV response of n-doping and p-doping of poly(decyl-thiophene) monolayers. This material is available free of charge via the Internet at http://pubs.acs.org.

LA026555K

(44) Israelachvili, J. N. *Intermolecular and surface forces*, 2nd ed.; Academic Press: New York, 2000; p 327.